Proceedings of the 15th International Heat Transfer Conference, IHTC-15
August 10-15, 2014, Kyoto, Japan

IHTC15-9593

MODELING THE THERMAL ENVIRONMENT IN AN OPERATING ROOM

Senhorinha F.C.F. Teixeira[1*], Nelson N.J.O. Rodrigues[1], Alberto S. Miguel[1], Ricardo F. Oliveira[2], José C.F. Teixeira[2], João S. Baptista[3]

[1]CGIT, University of Minho, Azurém, 5480 Guimarães, Portugal
[2]CT2M, University of Minho, Azurém, 5480 Guimarães, Portugal
[3]PROA, CIGAR, LABIOMEP, Faculty of Engineering, University of Porto, Porto, Portugal

ABSTRACT

Comfort is important in everybody's lives, as it is not only a health subject, but also a productive issue. As environmental conditions differ accordingly to the space use, there is a direct influence of this space on human comfort. The Heating Ventilation and Air Conditioning (HVAC) Systems are a crucial way to obtain the expected air quality levels in the interior of buildings and to achieve thermal comfort. These systems ensure air renewal, pressurization, temperature control, and air humidity, being of utmost importance in healthcare facilities. Providing thermal comfort conditions and good air quality, especially in operating rooms, is a difficult task, as the environmental conditions should be suitable for medical staff performance and for patient safety, as well. In the current study, a Computational Fluid Dynamics model was developed and coupled with a thermoregulatory model of the human body to describe the fluid flow, heat transfer and mass transfer between the ventilation air and a human manikin inside an operating room. The CFD simulation solves the heat, mass and momentum conservation equations in the computation domain using a finite volume discretization method, in the ANSYS © environment. The interaction between the body and the environment is determined by the thermoregulatory model, which includes temperature and the moisture diffusion through the cloth fabrics. The combination of the human body and space ventilation models allows evaluating the influence of the main thermal comfort variables on the calculation of comfort index, such as, the PMV.

KEY WORDS: Computational methods, Convection, Thermal comfort

1. INTRODUCTION

Comfort is a complex subject. It involves not only physical variables and models but also subjective concepts. Thermal comfort is defined by the American Society of Heating, Refrigerating and Air-conditioning Engineers (ASHRAE) as "the condition of the mind in which satisfaction is expressed with the thermal environment" [1]. This makes it difficult to get the same thermal perception in the same environment because that varies with each occupant [2].

Thermal comfort is also a productive issue, because people spend on average 90% of their lives indoor, where all aspects of human life (working, sleeping, studying, playing…) take place. Thus, it is vital to provide safe, healthy and comfortable conditions in buildings [3].

As environmental conditions differ accordingly to the space use, there is a direct influence of each space on human comfort. The correct calculation and optimization of the environment parameters are very important because they dictate the local comfort sensation which, in turn, affects the productivity and working performance of each person in the same environment [2]. The design of Heating, Ventilation and Air Conditioning (HVAC) systems has been a crucial way to obtain the desired air quality levels and to ensure thermal comfort in the interior of buildings. Because buildings can take approximately 40% of total primary energy consumed, their study and, consequently, the optimal design, are important.

*Corresponding Author: st@dps.uminho.pt

The HVAC systems are of utmost importance in healthcare facilities and, particularly, in operating rooms. A good design of ventilation and air conditioning systems provides a healthy and comfortable environment for patients and workers [4]. But, providing thermal comfort conditions and good air quality in operating rooms, is a difficult task, as the environmental conditions should be suitable for medical staff performance and for patient safety, as well. This means that studies concerning indoor thermal conditions are very important in defining, for instance, the satisfactory comfort temperature range in health care facilities. Thermal comfort is often assessed by the Fanger model, which is considered a good method for most of the cases. In fact, several authors comprehensively studied the thermal comfort in hospital facilities using this index [5], [6].

The Computational Fluid Dynamics (CFD) models are becoming an effective method for studying the fluid behaviour in complex situations [7], and, in this way, they have been applied in the thermal simulation of these spaces. Modeling of HVAC systems for velocity field and temperature distribution particularly at the vicinity of the human body has several difficulties. A common way to account for the human presence in the environment is to model that as a heat flux source [4]. The difficulty in modeling the human body is due to the complex geometric shape and its thermo-physiological properties, being important to include all these factors in the numerical simulation of the human body in a closed environment.

In the present study, a CFD model was coupled with a thermoregulatory model of the human body to describe the fluid flow, heat transfer and mass transfer between the ventilation air and a human manikin inside an operating room. In a first stage, a CFD simulation was carried out accounting for surgical lamps radiation heating, air humidity, airflow patterns and temperature distribution [6]. Subsequently, the influence of the environment in the human body was calculated by a thermoregulatory model which included temperature and the moisture diffusion through the cloth fabrics. Finally, these results of the human body temperature and humidity distributions were used as boundary conditions to the CFD model. In this way, one can assess detailed local boundary conditions for the human-environment interface and, therefore, calculate the effects of the thermal gradients in an individual. The computational model solved the heat, mass and momentum conservation equations in the computation domain using a finite volume discretization method, in the ANSYS © environment.

The main results of velocity, temperature and humidity are presented and discussed. The combination of the human body variables and the developed CFD model will allow evaluating the influence of the main thermal comfort variables on the calculation of PMV index values for the entire domain. Although, PMV is a comfort index that scales a subjective issue, it uses the average of the environmental conditions that surround the human body. The main question is that comfort does not only depend of the environment average values. Situations of local thermal discomfort due a cooler or hotter body part exist. This coupled computational model would improve the environment prediction at the skin surface. In this way, it would be possible to verify possible discrepancies between body regions.

2. CFD MODEL

The CFD model includes a set of equations that govern the conservation of mass, momentum and energy to compute fluid flow distribution and energy transport in the domain. A radiation model, a species model for a simplified air mixture and a turbulence model are also included.

Mass conservation implies that the mass entering a control volume equals the mass flowing out, creating a balance between input and the output flows for a certain volume. This concept is mathematically expressed by eq. (1), assuming constant fluid properties:

$$\nabla \cdot \vec{v} = 0 \tag{1}$$

where $\vec{v}$ represents the velocity vector.

Momentum conservation can be expressed by the rate of change of the momentum of a fluid's particle, and it is equal to the sum of the acting forces on the fluid (Newton's 2nd law). This principle can be described by eq. (2):

$$\nabla \cdot (\rho \vec{v} \vec{v}) = -\nabla p + \nabla \cdot \left[\mu \left(\nabla \vec{v} + \nabla \vec{v}^T \right) \right] + \rho \vec{g} \tag{2}$$

where $\vec{v}$ represents the velocity vector, μ represents the viscosity, ρ density, p represents static pressure, $\vec{g}$ represents gravitational acceleration [8].

For the turbulence modelling, a low-Reynolds number model proposed by Menter [9], the *k-ω* Shear Stress Transport (SST) was used. It was selected due to its precision and stability for predicting the fluid behaviour close to boundaries and heat transfer surfaces [10]. It combines the *k-ε* and the *k-ω* models using a blending function and applies them according to their performance. Thus, in the near wall regions, the SST model activates the *k-ω* model and, for the rest of the flow domain, the *k-ε* model is selected. This model was previously used for indoor airflow simulations obtaining accurate results [10], [11]. The extensive description and explanation of the SST *k-ω* model can be found elsewhere [8], [9].

The energy equation specifies that the rate of a particle's energy change equals the sum of heat rate added to the fluid particles and the work made into the particle [4]. The equation can be written as eq. (3):

$$\nabla . (\vec{v}(\rho E + p)) = \nabla . \left(k_{eff} \nabla T \right) + S_h \tag{3}$$

where k_{eff} represents the effective thermal conductivity, $\vec{v}$ represents the velocity vector, T represents the temperature, E represents the energy and S_h represents the source term for the energy equation.

Regarding the radiation in the operating room, the surface-to-surface (S2S) radiation model was used. This one implies the usage of a geometric function, "view factor", to calculate the energy transfer between the surfaces. It depends on the surface's area, distance between them, and reflective angle of orientation. This model is described thoroughly elsewhere [8].

The convective transport and diffusive mixing of chemical species were included in the simulation, by solving a conservation equation for each species. [8]. The fluid in the domain was considered as a typical mixture of H_2O, O_2 and N_2, being introduced in the room through the supply grille in the ceiling, with different mass fractions of each chemical component, according to their corresponding concentration.

To define the model completely, appropriate boundary conditions are required at each boundary segments of the computational domain. For the definition of the human body boundary, the interaction between the body and the environment (fluid inside the room and walls temperature) is determined by a thermoregulatory model. In this, the body is divided into 16 distinct parts. Part 1, which represents the lungs-heart where metabolic heat is generated, is considered as a unique system while all the other 15 parts are divided into three layers: core, shell and skin. Each layer has a uniform temperature and within each part exchanges are between the core and the shell and between this and the skin. In order to simulate a naked body, 46 ordinary differential equations describing the temperature variation along the time are solved. These equations describe the heat exchange by conduction due to the blood flux in the core and shell, heat changes due to the metabolism, the breading, the sweat produced in the shell layer and passing the skin layer, and finally, by the evaporation occurring at the skin surface. When the body part is naked, heat exchanges to the surrounding air by convection, radiation and evaporation.

Each one of the 15 parts (2-16) of human body can be covered with up to two layers of clothing. When the body part is covered (i.e., when the body is clothed), skin exchanges heat with the first layer of clothes and

the last layer exchanges by convection and radiation with the air. The model also includes the moisture diffusion through the cloth fabrics. Assuming that in the present study, a surgeon was simulated dressed, with only the head and the hands not covered, a system of 94 differential equations is solved, including 24 equations to calculate the water vapor density variation along the time, in the cloth layers. Full details of the model can be found elsewhere [12].

A main program solves all the balance equations numerically, using the Runge-Kutta-Merson method, implemented in a Fortran computer code. The initial temperature values in all body parts and layers (core, shell, skin and cloth) and the water vapour concentration at the cloth layers in all covered body parts are given and can be introduced by the user.

The CFD simulation process was carried out using the ANSYS™ Workbench platform to develop the mesh, run the CFD solver and the post-processing of the results.

3. NUMERICAL MODEL SETUP AND SOLUTION

A typical surgical room from a local hospital of dimensions L: 6.8 m × W: 5.6 m × H: 2.7 m is simulated which is approximated to a rectangular parallelepiped shape as shown in Fig. 1. Two surgical lamps and an operating table in the center of the room were also included. The air supply grille in the ceiling (simplified to forty eight rectangular diffusers) and the six exhaust grilles (two different types) dimensions were measured at the hospital. In the model, two rectangular ceiling lamps and an X-Ray board in the wall were also included.

For engineering purposes, some assumptions were implemented in the original geometry. One concerned the shape of the air supply diffuser, which was assumed to be rectangular although the actual air supply in the room had a round type grille mesh. This facilitated the definition of the computational grid in the vicinity of the air supply inlet. The same simplification was introduced in the exhaust zones. For the model simplification, a smaller number of air supply diffuser entries were also considered, although keeping the same area, for air flux and inertial sake.

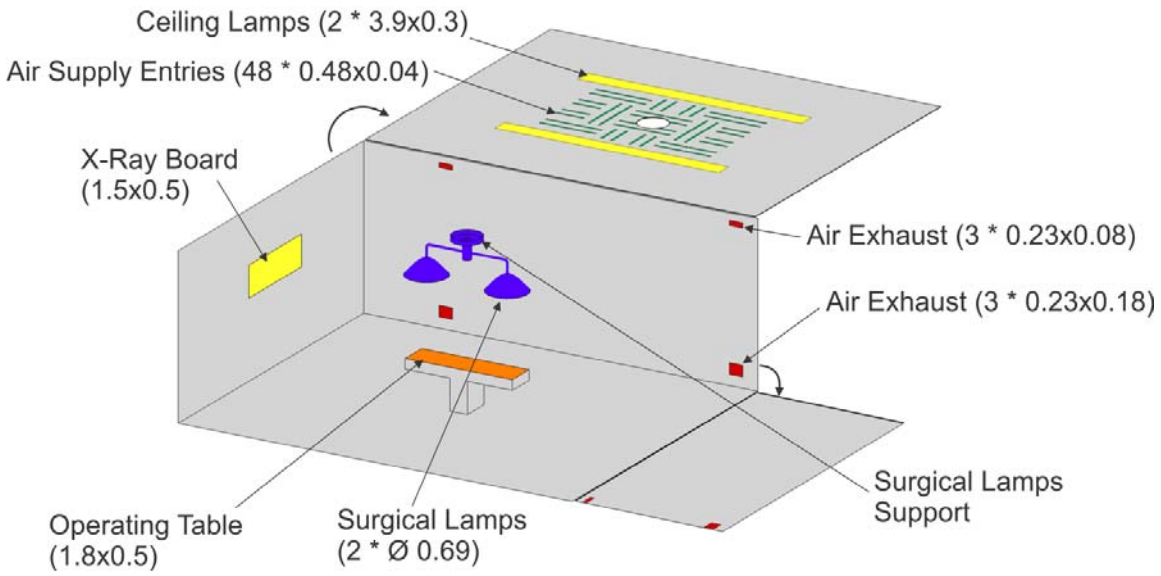

Fig. 1 Representation of the surgical room geometry.

To obtain the computational grid of the domain, the ANSYS™ software was used (see Fig. 2).

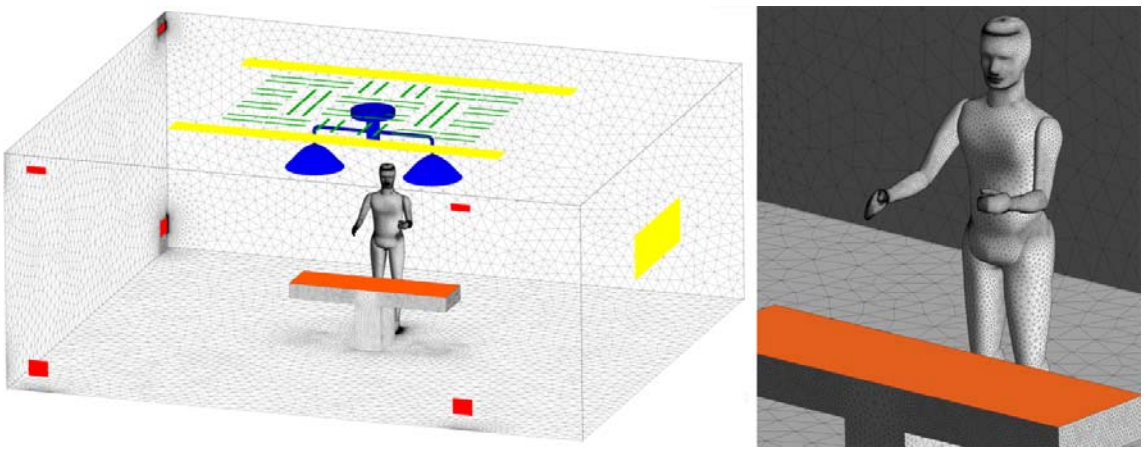

Fig. 2 Representation of the surgical room computational grid.

The domain is fully discretised by tetrahedral elements, using refinements in the most relevant boundary zones for accurate heat transfer calculation. Tetrahedral elements are more apropriate to match the complex surfaces of the human body with various elements of the room. An advanced size function that accounts for the proximity and curvature of the geometry was implemented.

To investigate the grid accuracy, 3 different grids of approximately 3, 5 and 8 million cells were evaluated. For each grid, the apparent order of the Grid Convergence Method (GCI), p, is calculated by Eq. 4 and 5.

$$h = \left[\frac{1}{N} \sum_{i=1}^{N} (\Delta V_i) \right]^{1/2} \tag{4}$$

where ΔV_i is the volume of the ith cell and the N is the total number of cells used [13].

$$\begin{aligned} p &= \frac{1}{\ln(r_{21})} \left| \ln\left| \varepsilon_{32} / \varepsilon_{21} \right| + q(p) \right| \\ q(p) &= \ln\left(\frac{r_{21}^{p} - (1 \cdot \mathrm{sgn}(\varepsilon_{32} / \varepsilon_{21}))}{r_{32}^{p} - (1 \cdot \mathrm{sgn}(\varepsilon_{32} / \varepsilon_{21}))} \right) \end{aligned} \tag{5}$$

$\varepsilon_{32}=\phi_3-\phi_2$, $\varepsilon_{21}=\phi_2-\phi_1$, and ϕ_k is the solution on the kth grid, being $h_1<h_2<h_3$ and $r_{32}=h_3/h_2$, $r_{21}=h_2/h_1$. The absolute velocity along a vertical line in the middle of the operating theatre was selected as the control variable ϕ. The local order of accuracy p ranges from 0.2 to 38.17, with a global average of 7.1, which is a good indication of the application of the hybrid method for that calculation. The approximate relative error is calculated by

$$e_a^{21} = \left| \frac{\phi_1 - \phi_2}{\phi_1} \right| \tag{6}$$

which can be used to assess the fine grid convergence index, GCI, for the finer grid

$$\mathrm{GCI}_{fine}^{21} = \frac{1.25 e_a^{21}}{r_{21}^{p} - 1} \tag{7}$$

GCI is a measure of the numerical uncertainty. This was found to be below 1.2%.

Table 1 lists the boundary conditions assumed in the computational simulations. For instance, at the air supply location, the data for the boundary condition was measured using a Brüel & Kjær indoor climate analyzer Type 1213. This is a device with several sensors that allows for the measurement of surface and air temperature, air velocity, relative humidity and radiative temperature in a confined environment. The air supply was defined as a velocity inlet condition, supplying the fluid at a constant velocity and temperature, which was considered a mixture of species for humidity assessment purposes. From the experimental data, some ventilation parameters were calculated. The Air Change per Hour (ACH) was found to be around 20 [14], the airflow rate was 2084 m^3/h corresponding to 55 $m^3/m^2/h$ [15]. At the inlet section, the turbulence intensity was defined as a function of the Reynolds number based on the hydraulic diameter.

Table 1 Boundary conditions assumed for the calculations.

Location	Boundary type	Material	Physical property	Value
Air Supply	Velocity Inlet	-	Velocity Temperature Humidity Hydraulic diameter Turbulence intensity	0.65 m/s 21.4 ºC 47.0 % 73.85 mm 5.81 %
Air Exhaust	Pressure Outlet	-	Gauge pressure	5.0 Pa
Walls, floor and ceiling	Wall	Concrete	-	Adiabatic
Ceiling Lamps	Wall	Glass	Heat Flux Area	50.0 W 2.34 m^2
Surgical Lamps	Wall	Glass	Heat Flux Area	260.0 W 0.75 m^2
X-Ray Board	Wall	Glass	Heat Flux Area	50.0 W 0.81 m^2
Surgical Lamps Support	Wall	Aluminium	-	Adiabatic
Operating Table	Wall	Cloth	-	Adiabatic

A pressure outlet condition on the air exhaust boundary guaranteed a positive pressure (5 Pa) in the room, assuring the ASHRAE standard [14]. It was also considered that the external walls of the domain do not perform a significant role in the heat transfer, being defined as adiabatic although the concrete material properties were applied (listed in Table 2) [16-17]. For the lamps in the room (ceiling, X-Ray board and surgical lamps), it was assumed that they had the thermal properties of the glass to simulate more precisely the radiant thermal flux. The material from the surgical lamps support was defined as aluminum. For the surface of the operating table, the properties of clothing were assumed once that surface is covered by bed sheets.

Table 2 Physical, thermal and radiative properties of the boundary materials.

	Density (kg/m^3)	Specific heat capacity (J/kg.K)	Thermal conductivity (W/m.K)	Surface emissivity
Concrete	2400	750	1.70	0.85
Glass	2600	840	1.05	0.93
Aluminium	2720	871	202.40	0.10
Cloth (cotton)	1500	1200	0.16	0.77
Skin	1200	7579	0.21	0.97

In order to define the boundary conditions for the human manikin, a preliminary solution for the velocity field was obtained assuming the dummy as a simple adiabatic wall. All the other boundary conditions (walls, heat sources, inlet velocity and outflows) were already defined. This simulation provided the data of the temperature field surrounding the human dummy. This temperature, obtained by post-processing the CFD results, was calculated by averaging the data over a volume centered in the dummy. For this purpose, a 1 m radius sphere was assumed. The average temperature surrounding the dummy was then used as an input to the thermoregulatory model of the human body.

For this study, a surgeon was simulated dressed using a long sleeve shirt and a surgical apron F-1, corresponding to C cloth configuration presented in the work of Konarska and collaborators [18]. For the surgeon, a metabolic rate of 1.93 Met (Metabolic Equivalent of Task = 58.2 W/m^2) and a clothing insulation value of 0.95 Clo (Clothing insulation = 0.155 $K.m^2/W$) were considered. These values were obtained from a survey made on the personnel working on this operating room, subsequently validated by direct comparison with data from the literature [18-19].

The results for the various parts of the human body were calculated using the thermoregulatory model, after a stabilization period (1 hour), and they are listed in Table 3. These data were used as the temperature boundary condition at the human dummy for Fluent™ final simulation. Subsequently, and considering a 65% relative humidity for the human skin, the H_2O mass fraction was calculated in the air at the vicinity of the human dummy. The humidity (65%) was assumed constant and all the other configuration parameters are kept as described previously.

Table 3 Boundary conditions for the human dummy.

Location	Boundary type	Material	Temperature
Torso and Belly	Wall	Cloth	31.95 ºC
Arms and Forearms	Wall	Cloth	30.17 ºC
Hips	Wall	Cloth	31 ºC
Legs	Wall	Cloth	30.97 ºC
Feet	Wall	Cloth	30.53 ºC
Head	Wall	Skin	34.35 ºC
Hands	Wall	Skin	34.21 ºC

The CFD simulation was carried out in a steady state, and the boundary conditions were assumed to be constant through time. The SIMPLE algorithm scheme for the pressure-velocity coupling was used. For spatial discretization of the pressure the Standard scheme was applied, while for the momentum, k, ω, species and energy, the Second Order Upwind scheme was selected. Solutions were obtained iteratively and different values have been tested for the convergence criteria. The convergence was accepted when the residuals for pressure, momentum, k, and ω were below 1E-4, and for the energy and species were below 1E-6 [6].

4. RESULTS AND DISCUSSION

The main CFD environment variables fields for the surgical room are now presented. They are represented as contours of velocity magnitude, temperature and relative humidity, drawn in the two perpendicular planes bisecting the dummy.

Fig. 3 and 4 show the contours for the absolute velocity field at the *xz* and *yz* plane, respectively. In both cases, it is easy to notice that, as expected, a zone of higher downwards velocity is located in the center of the room (i.e. above the operating table).

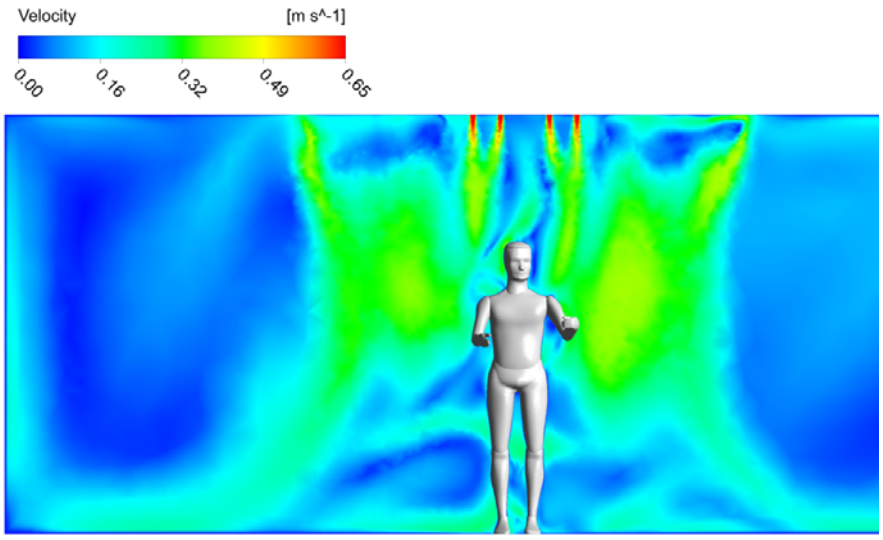

Fig. 3 Velocity distribution at a *xz* plane.

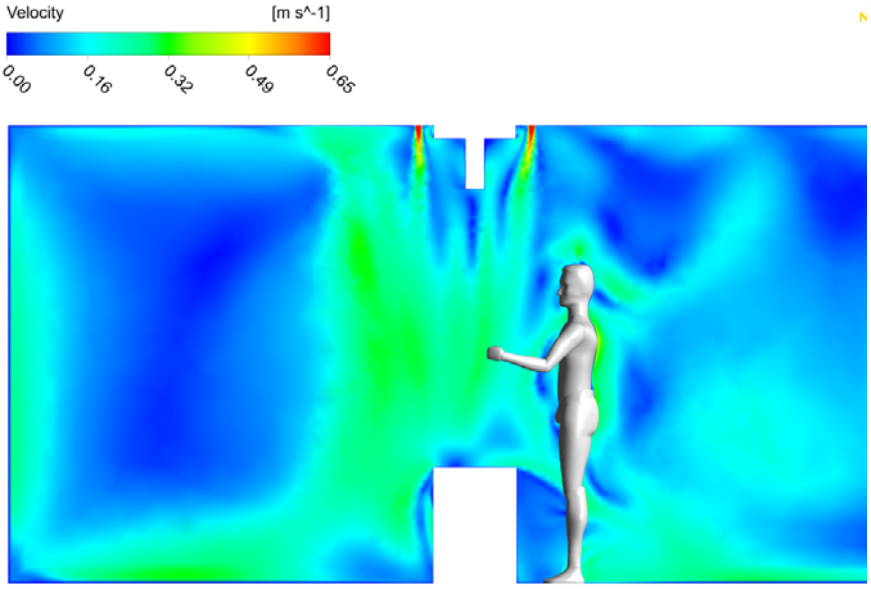

Fig. 4 Velocity distribution at a *yz* plane.

The velocity in the vicinity of the operating table is in the order of magnitude of 0.3 m/s, above the acceptable criterion of 0.2 m/s [20]. Such high velocity is due to the high inlet velocity at the ceiling openings. On the other hand, the air far from the centre of the room is nearly stagnant with a velocity close to zero. This means that the ventilation system is able to refresh the area above the operating table with more efficiency than the region close to the walls. It is also noticeable the influence of the human body as a thermal source. It is evident that by taking into account the actual body surface temperature, the velocity field inside the room can be disrupted. The same patterns can be observed in Fig. 4. The upwards flow along the body yields flow separation near the dummy's right shoulder causing a non-symmetry pattern. A previous work [21] modelling the flow in a room, shows similar results for the human presence in a room ventilation field.

The temperature field shows a pattern similar to that of the velocity magnitude. The thermal plume around the human body is clearly identified in Fig. 5 and 6, where the temperature distribution is presented at the *xz* and *yz* plane, respectively.

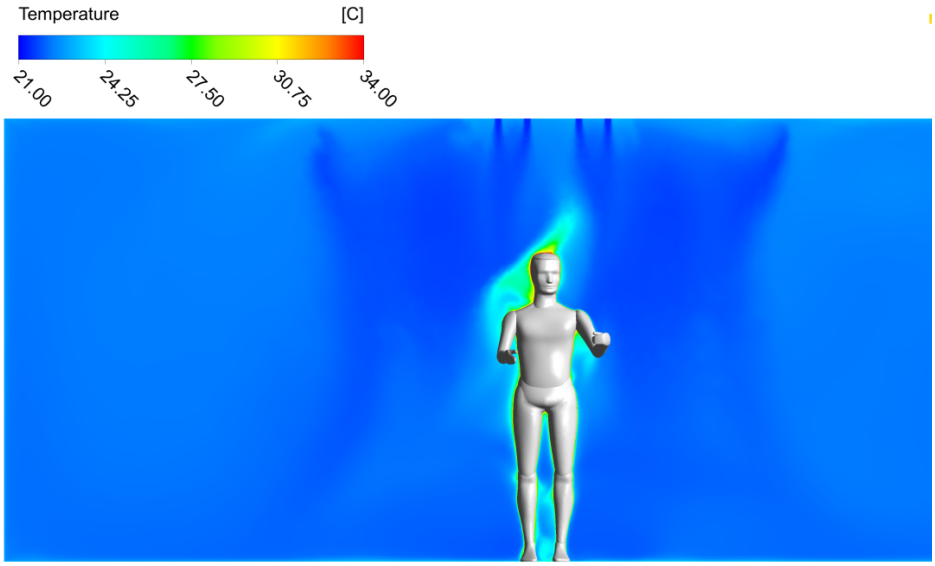

Fig. 5 Temperature distribution at a *xz* plane.

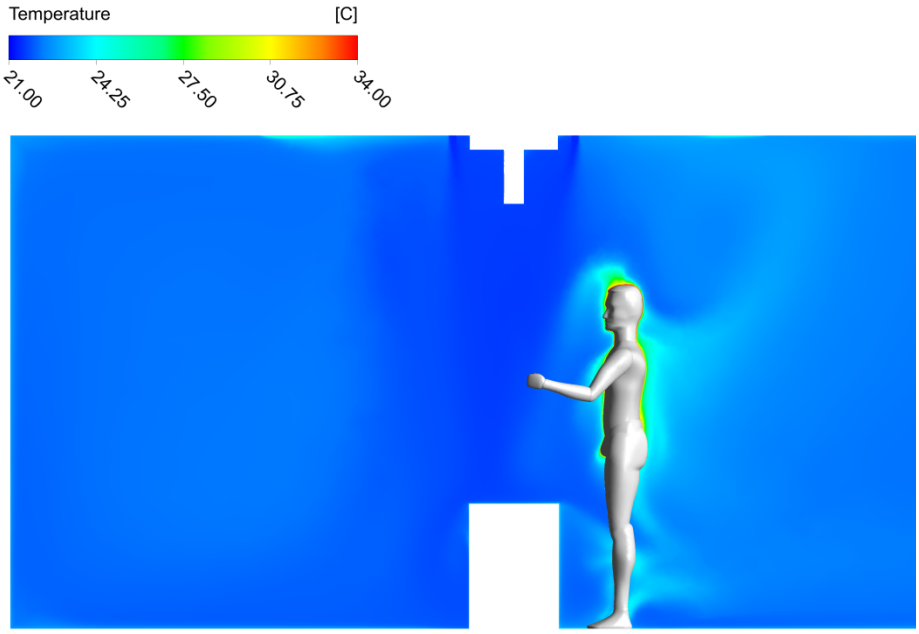

Fig. 6 Temperature distribution at a *yz* plane.

The temperature field ranges from a lower value of 21.0 ºC at the air supply to a maximum value of 34.35 ºC in the human dummy surface (truncated at 34.0 ºC for representation purposes). This behavior is expected as well the colder air moving in the centre of the room, descending from the air supply onto the table surface, as previously discussed. The heated air zones are found next to the surgical lamps and human dummy, mainly due to its high heat fluxes.

The influence of the human dummy on the ambient temperature profile can be observed in Fig. 7. The data was retrieved at an axis across the width of the room at z=2 m and x=3.55 m; that is above the human manikin. The results show the influence of the convective plume driven by the body surface.

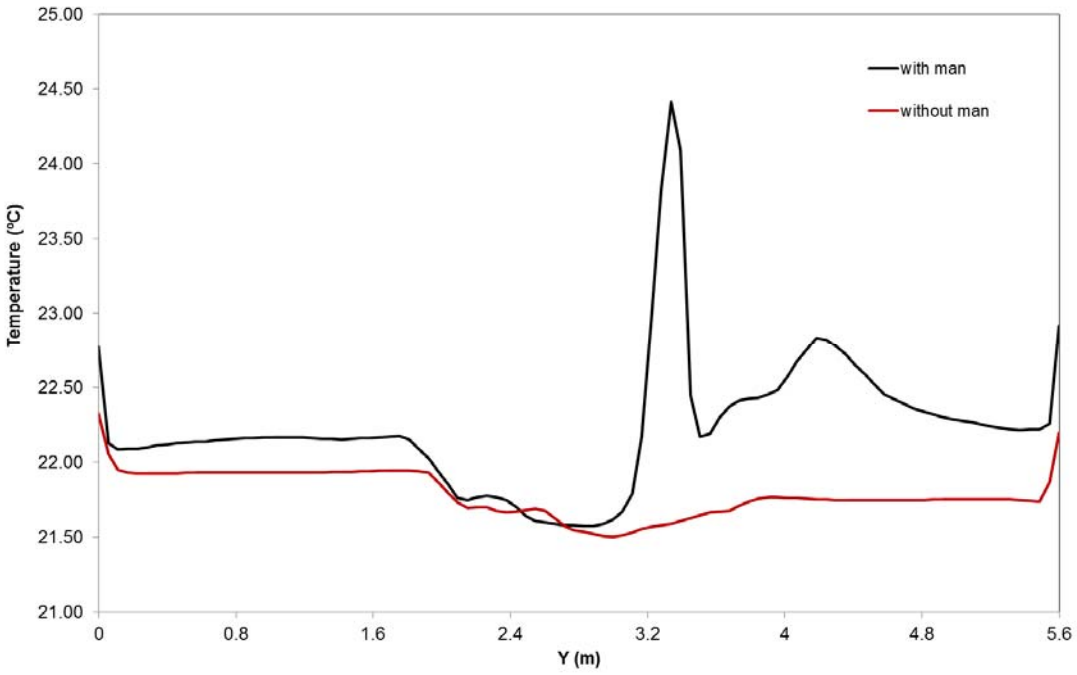

Fig. 7 Temperature profile across the operating room.

Relative humidity field are represented in Fig. 8 and 9, at the *xz* and *yz* plane, respectively. The values range from 33% to 65% (constant value assumed at the human body surface). The domain average value for relative humidity is around 49%.

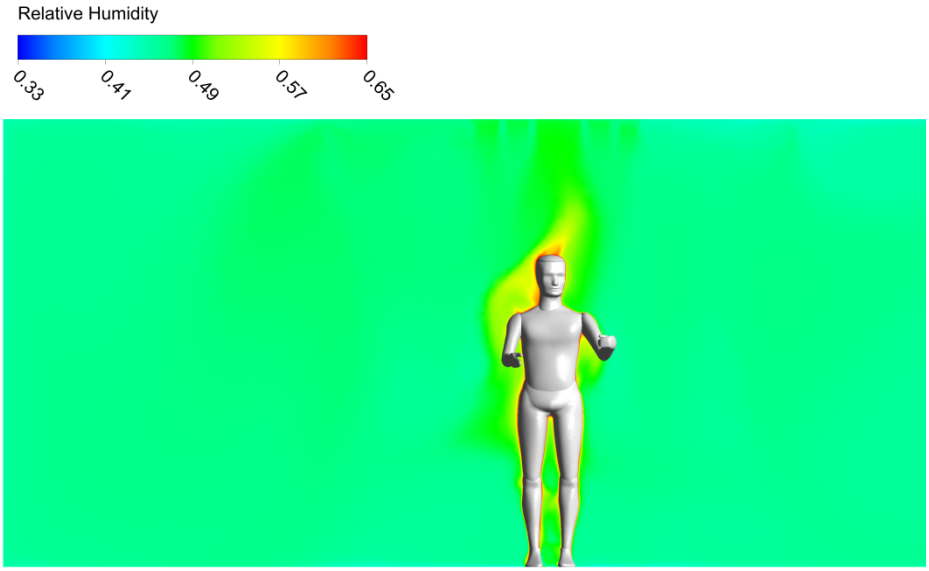

Fig. 8 Relative humidity distribution at a *xz* plane.

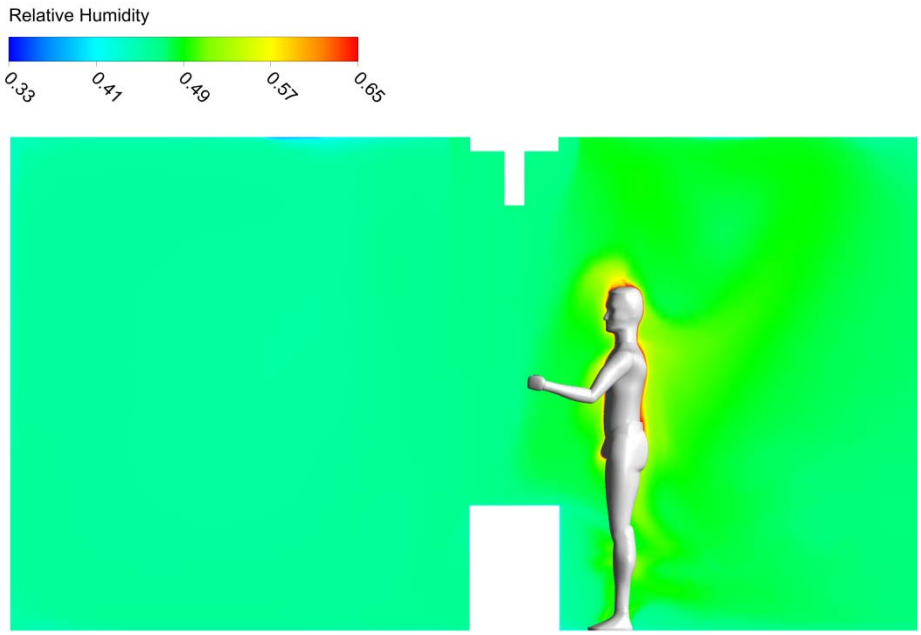

Fig. 9 Relative humidity distribution at a *yz* plane.

The maximum relative humidity is observed at the skin surface and that decreases with the distance from the body. It may be concluded that the body is indeed a moisture source. The pattern closely follows that observed for the velocity field. It is also possible to observe that the temperature and the mass fraction distributions are similar, which is in agreement with the principle that the higher the temperature, the higher the potential level of water vapor in the air.

6. CONCLUSIONS

The main objective of the present work is the use of a CFD model to compute the thermal evolution of an air-conditioning Portuguese orthopedic surgical room. Analyses were made at the air velocity, temperature and relative humidity fields obtained. In order to fulfill account with the human presence in the room, a thermoregulatory model is used to described the interaction of a surgeon (metabolic and cloth values) with the surrounding air. The boundary conditions were based on experimental measurements of temperature, air velocity and humidity at the inlet air ventilation supply.

The results seem very satisfactory as they simulated the expected trends. Using a simulated human body, divided into parts with different temperatures, seems important to give accurate fluid flow and moisture distributions in the room. The combination of the human body variables and the developed CFD model will allow evaluating the influence of the main thermal comfort variables on the calculation of PMV index values for the entire domain [6]. The inclusion of detailed data regarding the human surface (temperature and humidity) as a function of the metabolic rate and clothing is paramount to the accuracy of the calculations. It can quantify the main differences between patients and various workers at different places, inside the operating room.

Experimental work is now taking place during a surgical operation to allow the validation of the computational model. The simulation of a complete team of a surgeon, patient and nurse staff must be accomplished.

ACKNOWLEDGMENT

This work was financed by National Funds-Portuguese Foundation for Science and Technology, under Strategic Project and PEst-OE/EME/UI0252/2011 and also the PEst-C/EME/UI4077/2011.

REFERENCES

[1] ANSI/ASHRAE Standard 55, *Thermal Environment Conditions for Human Occupancy,* (2004).

[2] Djongyang, N., Tchinda, R., Njomo, D., "Thermal comfort: A review paper," *Renewable and Sustainable Energy Reviews*, 14, pp. 2626-2640, (2010).

[3] Hajdukiewicz, M., Geron, M., Keane, M.M., "Calibrated CFD simulation to evaluate thermal comfort in a highly-glazed naturally ventilated room," *Building and Environment*, 70, pp. 73-89, (2013).

[4] Ho, S. H., Rosario, L., Rahman, M.M., "Three dimensional analysis for hospital operating room thermal comfort and comtaminant removal," *Applied Thermal Engineering*, 29, pp. 2080-2092, (2009).

[5] Pourshaghaghy, A., Omidvari, M., "Examination of thermal comfort in a hospital using PMV-PPD mode," *Applied Ergonomics*, 43(6), pp. 1089-1095, (2012).

[6] Rodrigues, N.J.O., Teixeira, S.F.C.F., Miguel, A.S., Oliveira, R.F., Teixeira, J.C.F. and Baptista, J.S., "Thermal Comfort evaluation of an operating room through CFD methodology," *Proc. of the Occupational Safety and Hygiene Symposium – SHO 2013, pp. 411-416, CRC Press - Taylor & Francis, ISSN 2182-8482,* (2013).

[7] Versteeg, H. K. and Malalasekera, W., *An Introduction to computational fluid dinamics: The finit volume method,* Publisher, Longman Scientific & Technical, (1995).

[8] ANSYS, *ANSYS FLUENT Theory Guide*, Canonsburg, PA, USA: ANSYS Inc., (2011).

[9] Menter, F.R., "Two-equation eddy-viscosity turbulence models for engineering applications," *AIAA Journal*, 32, pp. 1598-1605, (1994).

[10] Zhai, Z.J., Zhang, Z., Zhang, W., Chen, Q.Y., N., "Evaluation of Various Turbulence Models in Predicting Airflow and Turbulence in Enclosed Environments by CFD: Part 1—Summary of Prevalent Turbulence Models," *HVAC&R Research*, 13, pp. 853-870, (2007).

[11] Stamou, A., Katsiris, I., "Verification of a CFD model for indoor airflow and heat transfer," *Building and Environment*, 41, pp. 1171-1181, (2006).

[12] Teixeira, S., Leão, C., Neves, M., Arezes, P., Cunha, A., and Teixeira, J., "Thermal Comfort Evaluation using a CFD Study and a Transient Thermal Model of the Human Body," *Proc. of Fifth European Conference on Computational Fluid Dynamics, ECCOMAS CFD*, (2010).

[13] Celik. I. B.; Ghia, U.; Roache, P. J., Freitas, C. J. "Precedure for estimation and reporting of uncertainty due to discretization in CFD applications," *Journal of Fluids Engineering*, 130(7), (2008).

[14] ASHRAE Standard 170P, *Ventilation of Health Care Facilities,* (2006).

[15] Balaras C.A., Dascalaki, E., Gaglia, A., "HVAC and indoor thermal conditions in hospital operating rooms," *Energy and Buildings*, 39, pp. 454-470, (2007).

[16] Kilic, M, Sevilgen, G., "Modelling airflow, heat transfer and moisture transport around a standing human body by computational fluid dynamics," *International Communications in Heat and Mass Transfer*, 35, pp. 1159-1164, (2008).

[17] Sun, Z., Wang, S., "A CFD-based test method for control of indoor environment and space ventilation," *Building and Environment*, 45, pp. 1141-1147, (2010).

[18] Konarska, M., Sołtynski, K., Sudoł-szopińska, I., "Comparative Evaluation of Clothing Thermal Insulation Measured on a Thermal Manikin and on Volunteers," *Fibres & Textiles in Eastern Europe*, 15, pp. 73-79, (2007).

[19] Zwolinska, M., Bogdan, A., "Impact of the medical clothing on the thermal stress of surgeons," *Applied Ergonomics*, 43, pp. 1096-1104, (2012).

[20] Drake, B., "Infection control in hospitals," *ASHRAE Journal*, 48, H12-H17, (2006).

[21] Cunha, A.M.F., Teixeira, J.C.F., Teixeira, S.F.C.F., "Computational fluid dynamics applicable to cloth design," *ASME Conf. Proc. IMECE2009, November 13-19, 2009, Lake Buena Vista, Florida, USA, Volume 2: Biomedical and Biotechnology Engineering, pp. 233-241, http://dx.doi.org/10.1115/IMECE2009-13042,* (2009).